PROJECT FINAL REPORT

Grant Agreement number: CS-GA-2009-255806

Project acronym: FUSDESOPT

Project title: Fuselage Design Optimization

Funding Scheme: Clean Sky

Period Covered: from 1-1-2010 to 1-7-2010
Actual date of completion: 1-4-2011

Name of the scientific representative of the project's coordinator, Title and Organization:

Dr. Andrew Barton, AOES
Tel: +31-71-5795535
Fax: +31-71-5721277
Email: andrew.barton@aoes.com

Executive Summary

The purpose of the FusDeOpt project was to use detailed numerical simulations to investigate possible mass savings on aircraft fuselage structures using Laser Beam Welding (LBW) technologies. Analyses were conducted for stinger-reinforced aluminium panels with a number of different stringer configuration and material options. A reference panel using conventional riveted aluminium construction was analysed, as well as a number of LBW options.

Analyses were first undertaken firstly using the traditional 'classical' techniques, and then a variety of Finite Element Method (FEM) models were analysed.

2D FEM analyses were conducted of pull-test specimens for a variety of welded stringer configurations. 3D FEM analyses were conducted for panel compression specimens, which exhibited complex failure modes involving panel buckling and local plasticity at the root of the stringers. The 3D analyses included SHELL element models and SOLID element models.

All FEM models included the effects of material nonlinearity, geometric nonlinearity (i.e. large displacements) and, in the case of the riveted panel structures, contact and gapping. Initial imperfections were included in the SHELL element models for the compression panels however the results showed that the effect of imperfections was always less than 2% of the ultimate strength. Thus, for the 3D SOLID element analyses, considering the high computational efforts required, no attempt was made to model initial imperfections.

The 2D pull-test specimens showed failure modes with almost pure tension in the weld seam. This differs from the 3D panel compression specimens which showed failure by lateral bending of the stringer root at a load weakened by plasticity in the weld seam (see Figure 5-5 of this report). The difference between these local failure modes means that the results of the 2D pull-test specimens cannot be directly used to predict the strength of the 3D compression panels.

The 2D results do however permit an assessment of the relative strength of the different materials and heat treating options of the welded joint, and it is likely that a design that performs well in the pull-test loading will also show good resistance to stringer rotation in 3D panel compression loading.

The SHELL element models have relatively few elements and thus provide a solution time of only a few hours on the typical modern computers used for this project. The SHELL elements are suitable for modeling global effects in the large regions of the panels, but the representation of the weld seam does not give sufficient accuracy for local failures.

The SOLID element models can provide sufficient accuracy for local failures, but this comes at a high computational cost, since it is impossible to predict in advance where the failure will occur. The high computational costs also make a thorough investigation of the effects of initial imperfections very time consuming.

Table of Contents

Summary description of context and objectives

1. Introduction

1.1. The Project

FusDesOpt (contraction of “Fuselage Design Optimization”) is the short hand name for the project “Numerical Simulation and Design Optimization of a Lower Fuselage Structure with Advanced Integral Stiffening” with the identifier GRA-01-017, which falls under the Green Regional Aircraft (GRA) Integrated Technology Demonstrator (ITD) of the European Commission’s Clean Sky programme. In late 2009 AOES prepared a successful proposal for the FusDesOpt project in response to the Clean Sky call SP1-JYI-CS-2009-01.

The FusDesOpt project manager is the Fraunhofer Institute for Material and Beam Technology (Fraunhofer IWS) based in Dresden, Germany. Fraunhofer IWS is developing new welding techniques for aircraft structures that are the subject of the FusDesOpt project.

1.2. Scope and Objectives

The main objective of this project was to use detailed numerical simulations to investigate possible mass savings on aircraft fuselage structures using Laser Beam Welding (LBW) technologies.Minimizing the weight of an aircraft design is essential for optimal payload performance and leads to reductions in fuel consumption, thus reducing the carbon emissions and reducing the operating cost. The subject of this project, being a fuselage structure subject to predominately static loads, which are mostly critical in compression and shear, is dominated by stiffness considerations, and in particular buckling stability.

Analyses were conducted for stinger-reinforced aluminium panels with a number of different stringer configuration and material options. A reference panel using conventional riveted aluminium construction was analysed, as well as a number of LBW options.

Analyses were first undertaken using the traditional ‘classical’ techniques, and then a variety of Finite Element Method (FEM) models were analysed.

Three different types of analysis were conducted

- Classical method using hand calculations on the reference structures (riveted) to determine the overall buckling behavior of the panel.
- 2D FEM for the weld area to simulate a stringer pull-off test
  Two different stringer configurations were analysed:
  - The L stringer (see Figure 1-4)
  - The U stringer (see Figure 1-5)

  Both stringer types were analyzed for two different materials and two different heat treatments
- 3D FEM for the complete panel
  The 3d FEM can be subdivided into a 3D model built up of shells and not accurately representing the welded zone and a full 3D model (using solid 3D models) that includes an accurate description of the weld zone. These 3D analyses are used to determine the influence of the LBW method on stability performance of the panel compared to its weight associated with the different configurations, materials and heat treatments.

The failure load of stiffened thin shell structures subjected to compression loads is quite sensitive to initial imperfections in the geometry, material properties or internal pre-load. Small variations in these parameters are unavoidable in any manufacturing process. The common practice to account for these effects is to analyze the structure with deliberately introduced imperfections scaled from buckling mode shapes of the ideal structure. In this report only the first buckling mode was considered for the imperfection analysis however a full justification would require a number of buckling modes.

The reference structure is shown in Figure 1-1, Figure 1-2, Figure 1-3 and Figure 1-4 (for the LBW stringer). The corresponding 3D FE- models are shown in Figure 1-6 and Figure 1-7.

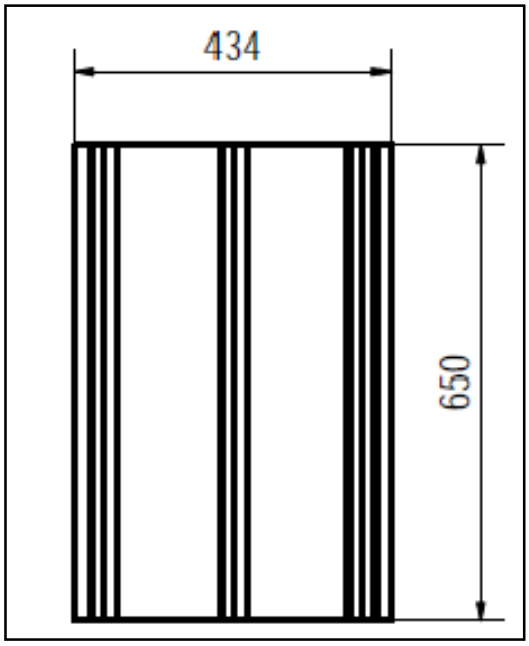

Figure 1-1 Reference Structure Plan View

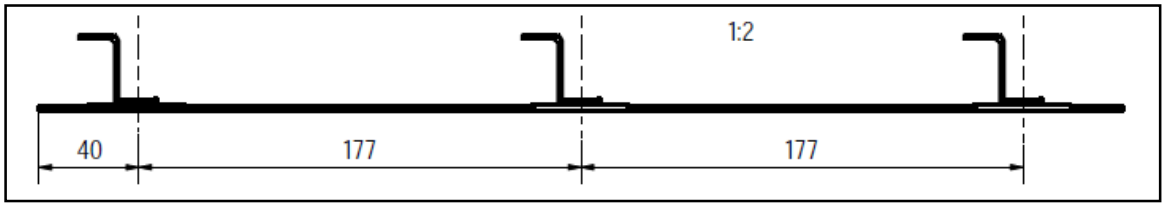

Figure 1-2 Reference Structure Section View

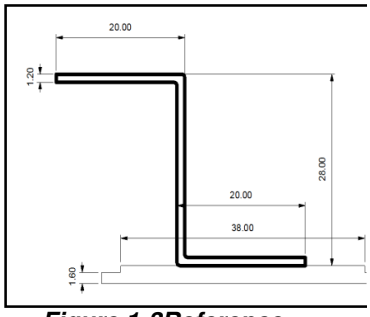

Figure 1-3Reference Structure Stringer Cross-Section

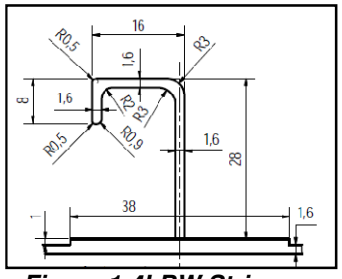

Figure 1-4LBW Stringer Cross-Section Detail

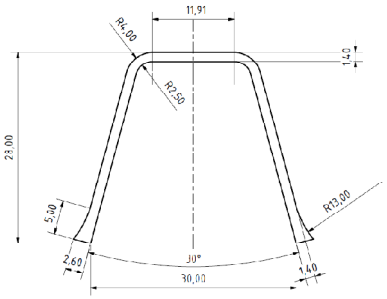

Figure 1-5: U-Stringer Top Hat Detail

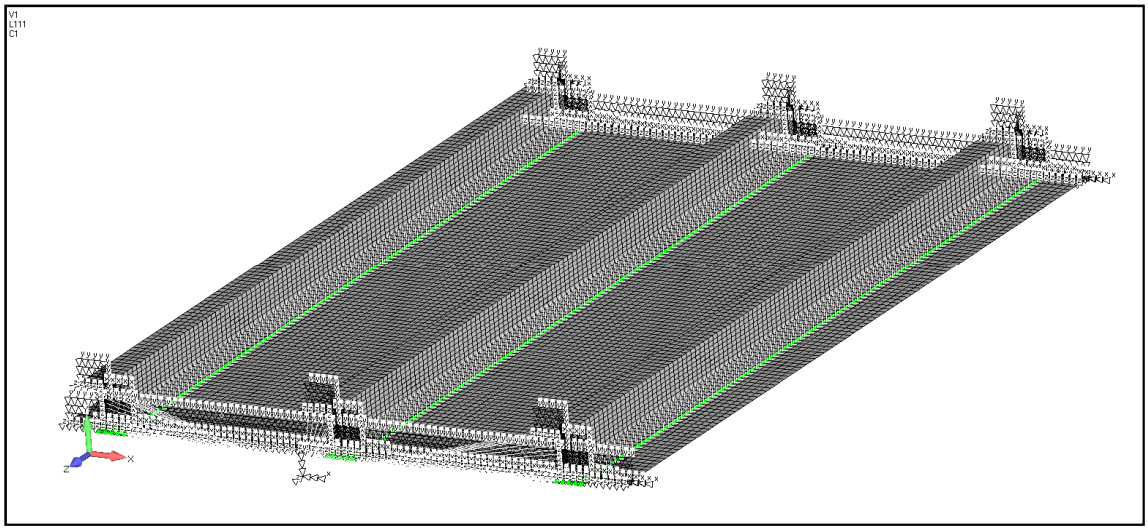

Figure 1-6 3D FEM Model of Reference Structure (using plate elements)

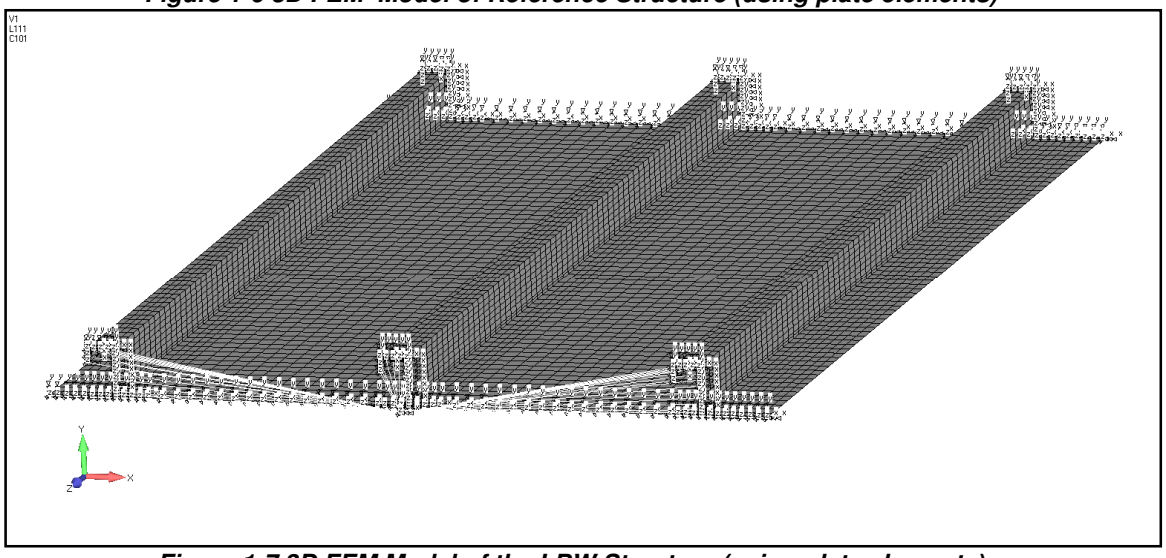

Figure 1-7 3D FEM Model of the LBW Structure (using plate elements)

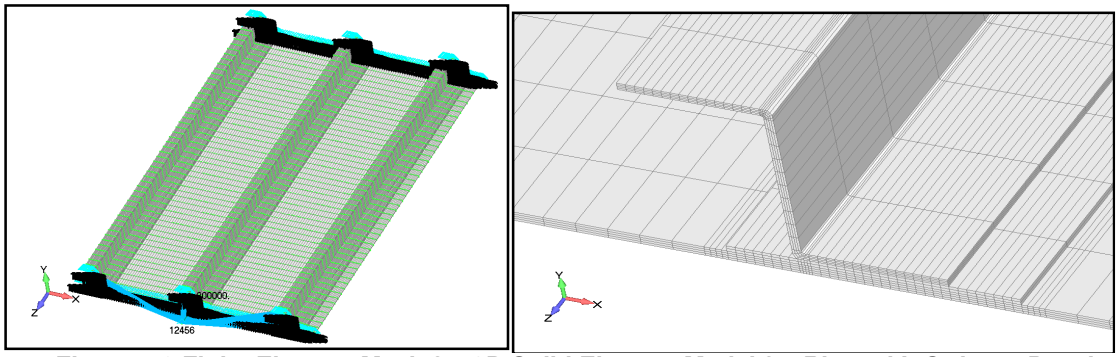

Figure 1-8 Finite Element Mesh for 3D Solid Element Model for Riveted L-Stringer Panel

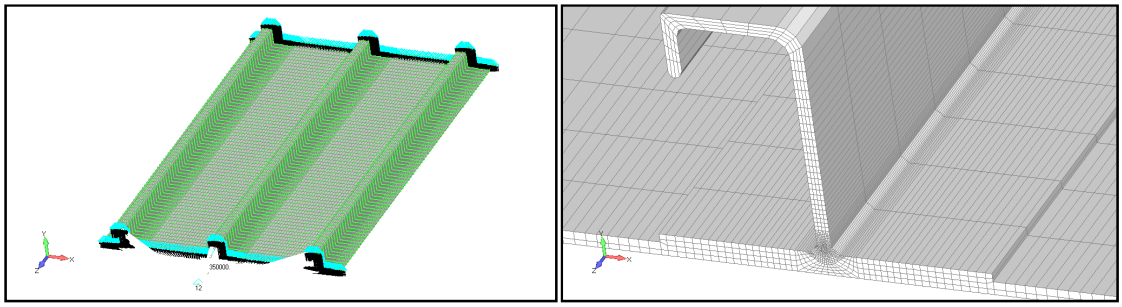

Figure 1-9 Finite Element Mesh for 3D Solid Element Model for Welded L-Stringer Panel

This report covers the work performed in the project. Table 1-1 summarizes the works undertaken in each Work Package (WP).

WP	WP Title	Analysis Methods			
		2D Pull-Off	3D Shell	3D Solid	3D Classical
1	Analysis of Reference Structure		Y		Y
2	Impact of LBW	Y	Y		Y
3	Solid Analysis of LBW Structure			Y	
4	Solid Analysis of Reference Structure			Y	
5	Analysis of U-Stringer	Y			

Table 1-1 Allocation of Work by WP

Main S&T results

2. Classical Analysis of Reference Structure

AOES undertook strength calculations using classical methods based on continuous panel theory, which assumes an infinitely wide panel with uniform stiffener spacing. This section shows the calculations for the Buckling Failure Load prediction for the reference structure, a riveted panel based on traditional aircraft manufacturing approaches.

2.1. Calculation Flowchart

The calculation procedure is shown in
Figure 2-1.

2.2. Summary of Classical Analysis of Reference Structure

The compression strength of the reference panel was found to be 140.3kN. The failure mode is crippling of the stringers. The calculated failure load includes an extra strength contribution from the skin directly adjacent to the stringers. Initial skin buckling occurs at a load of 21.7 kN, far below the failure load. Inter-rivet buckling was predicted at 127.1kN. The "effective width" of adjacent skin is 40.01 mm (this figure takes into account the effect of inter-rivet buckling).

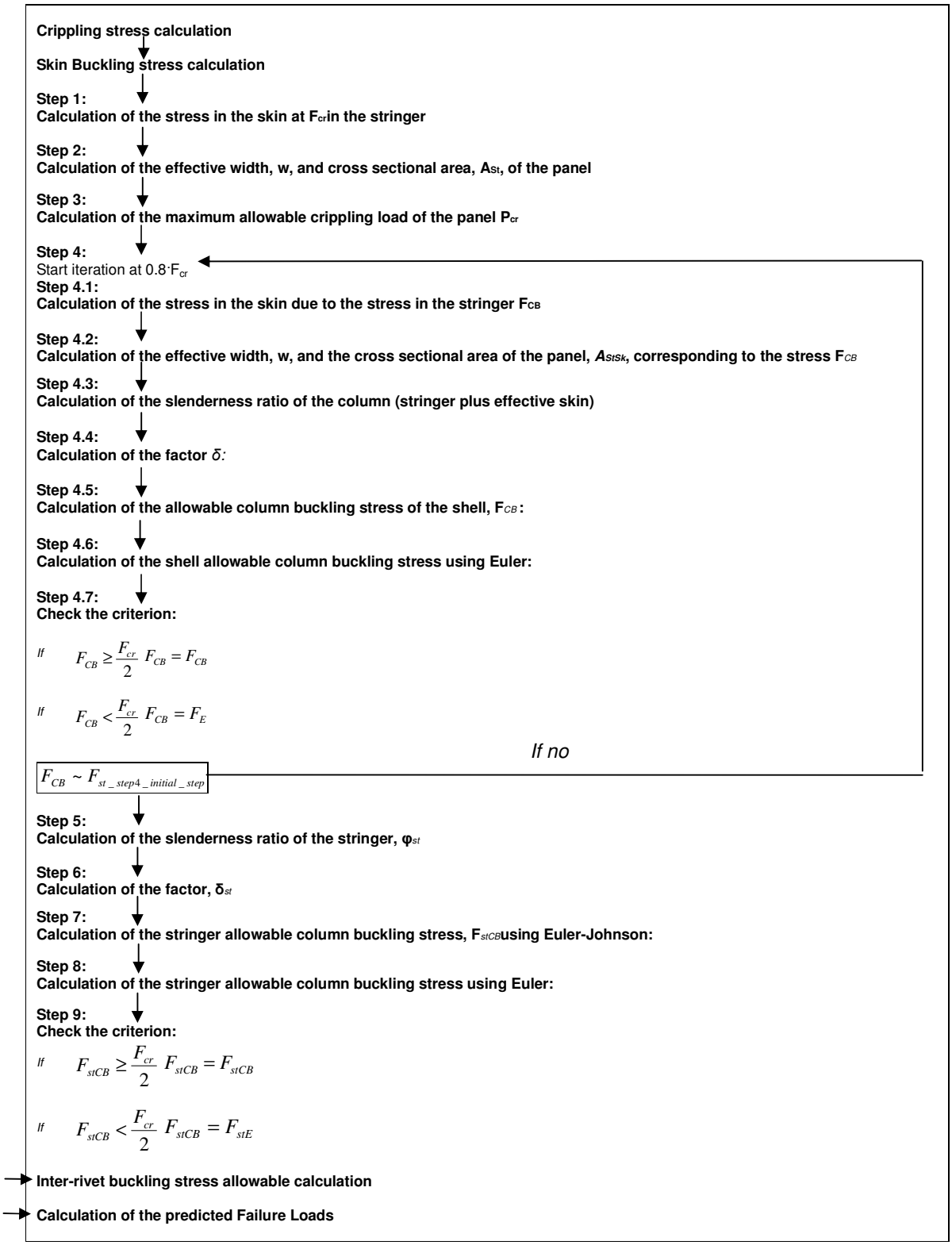

Figure 2-1 Procedure for the Analysis of Reference Structure by Classical Methods

3. 2D Pull-Test Analysis Results

Both in WP 2 and 5, a 2D analysis of the stringer pull of test was performed. In WP2 the analysis was of a T joint, in WP5 a U-type stringer was analysed.

3.1. 2D Analysis of T-joint

This chapter presents the results of the nonlinear static analysis of a number of T-joint pull test specimens representing a number of LBW stringer design options under consideration by Fraunhofer IWS.

3.1.1. FEM Model

The analyses were made using 2D plain strain elements, an approach that is suitable for long structures with constant cross-sectional properties.

The model was constrained in the vertical direction by roller supports located at four nodes on the skin located approximately 0.5mm from the fusion zone boundary. The vertical member was constrained to move only in the vertical direction. These constraints are shown in Figure 3-1.

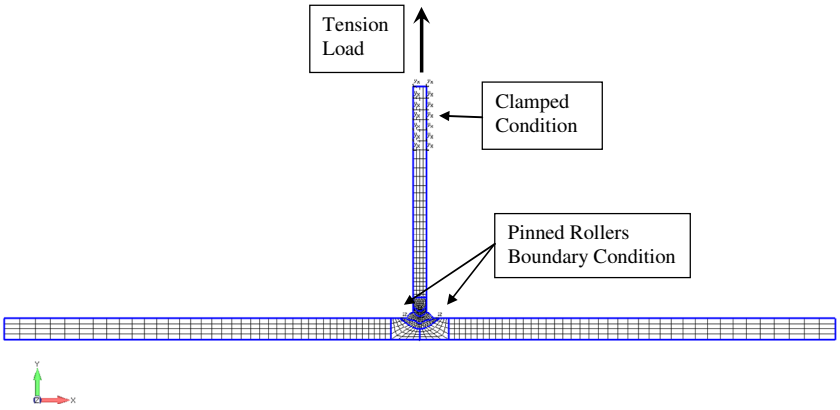

Figure 3-12D FEM Model of T-Joint Pull Specimen

The vertical member of the T-Joint was loaded with in the vertical upwards (tension) direction.

3.1.2. T-Joint Configurations

analyzed T-Joint options are shown in Table 3-1.

Material	Heat Treatment	Weld Type
Al-Li	as welded	1
Al-Li	as welded	2
Al-Mg-Si	PWHT	1

Table 3-1 T-Joint Configurations

Two different weld geometry types were requested by Fraunhofer IWS for the Al-Li / as welded option. Only Weld type 1 is shown here for better comparison with Al-Mg-Si / PWHT.

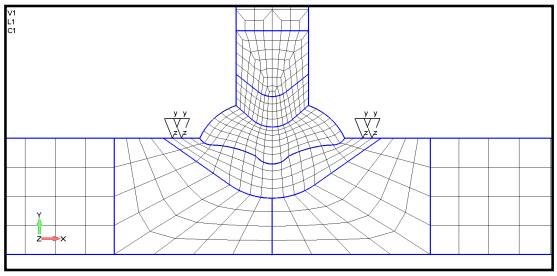

Figure 3-2 Weld Type 1

3.1.3. 2D FEM Results - Al-Li / as welded - Weld Type 1

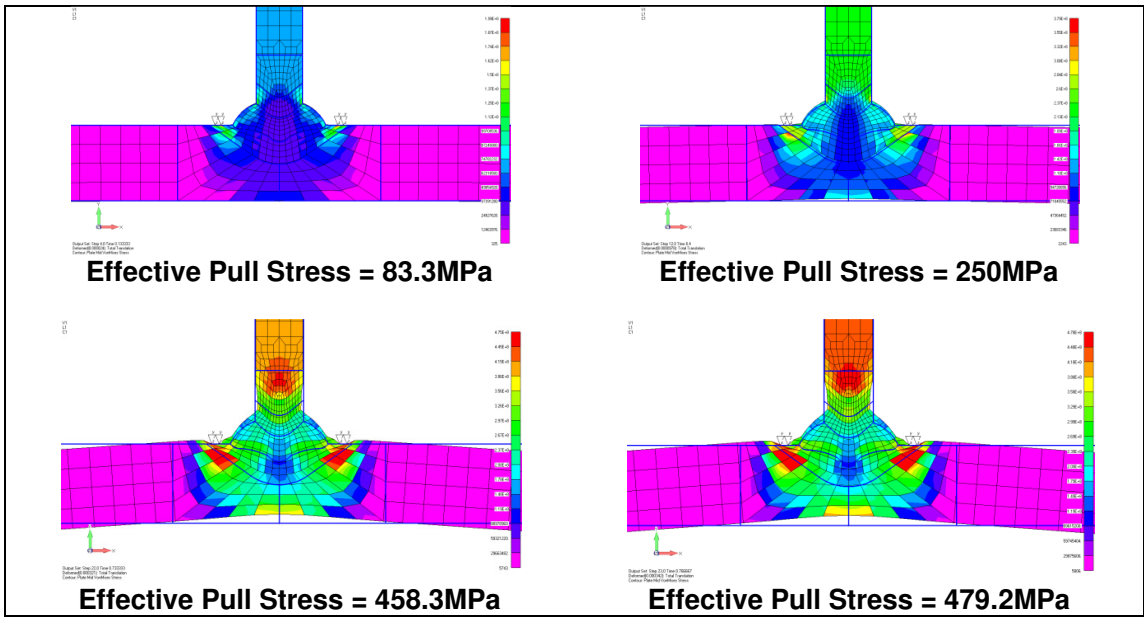

Figure 3-3Von Mises Stress Contour Plots - Al-Li / as welded – Weld Type 1

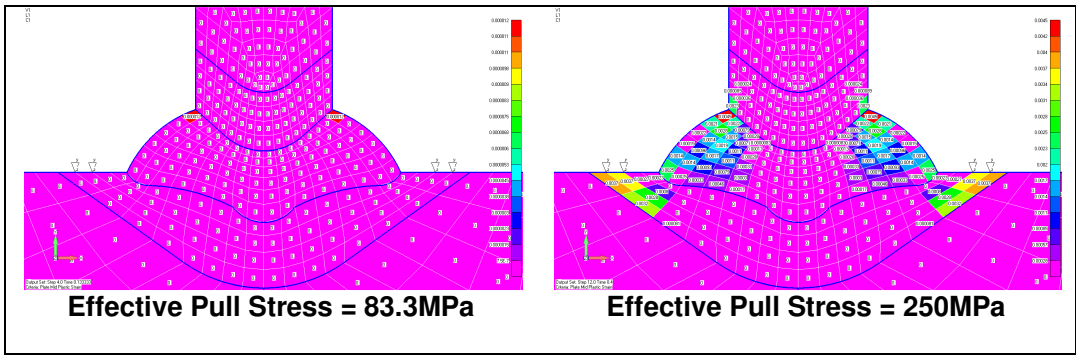

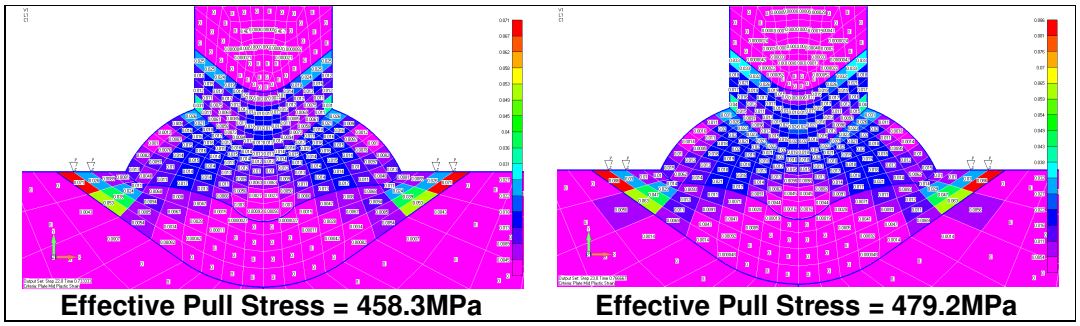

Figure 3-4Plastic Strain Plots - Al-Li / as welded – Weld Type 1

3.1.4. 2D FEM Results - Al-Mg-Si / PWHT

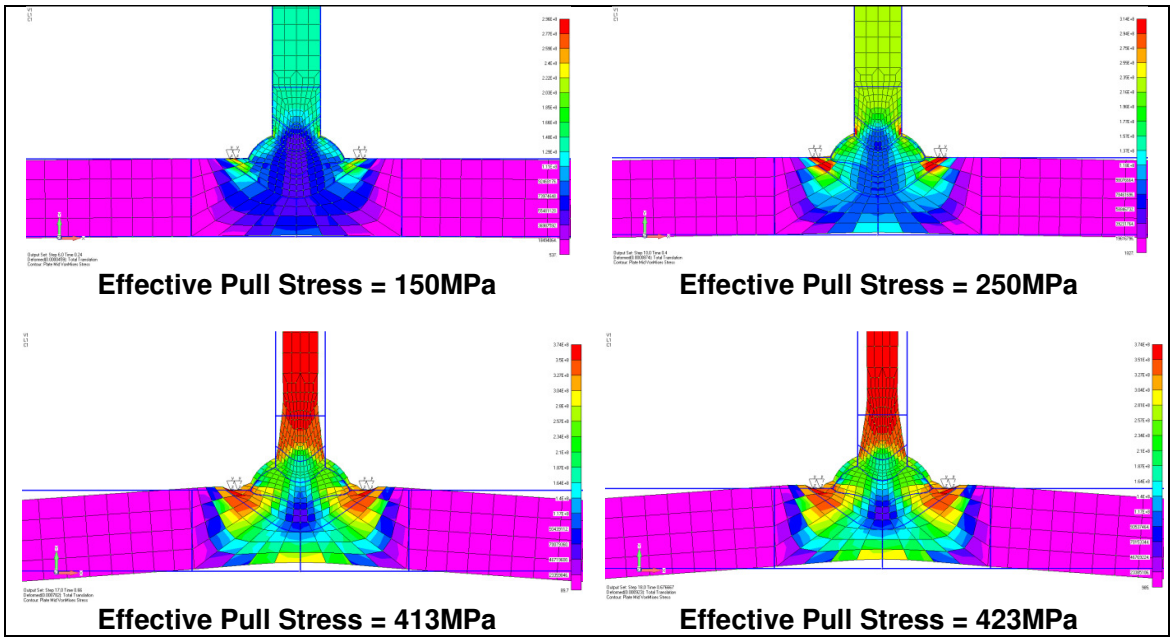

Figure 3-5Von Mises Stress Contour Plots - Al-Mg-Si /PWHT

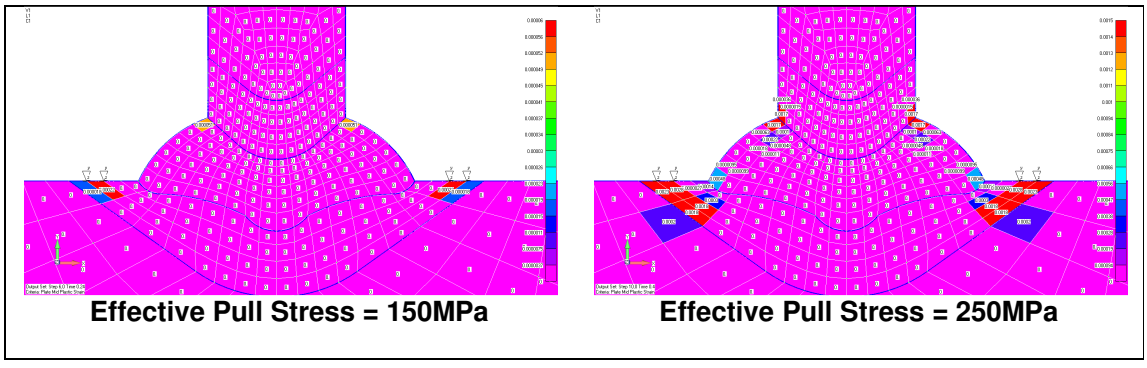

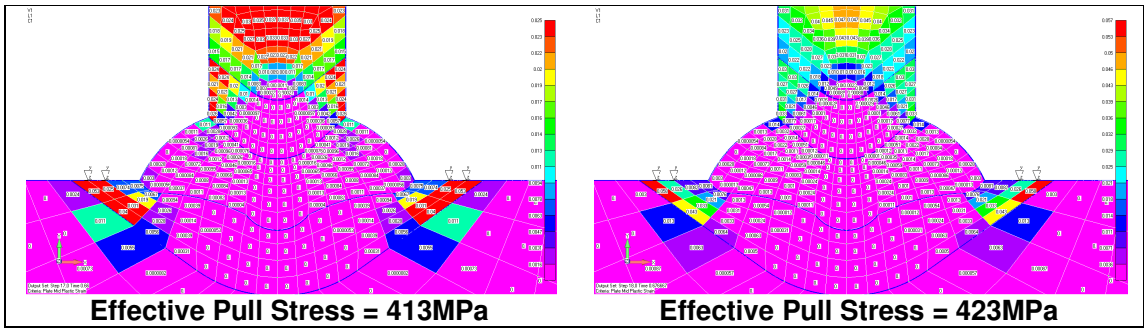

Figure 3-6Plastic Strain Plots - Al-Mg-Si / PWHT

3.2. 2D Analysis of U-Stringer

3.2.1. Configuration

This alternative welded stringer configuration was provided by IWS[2] for comparison with the L-stringer configurations analyzed in the previous work packages. It features a “U” shaped stringer profile (also sometimes called a ‘top-hat’ stringer).

Only 2D pull-off analysis was conducted for this stringer configuration, although it is likely that this configuration would perform quite well in 3D compression panel analysis.

3.2.2. Finite Element Mesh

The finite element mesh is shown in Figure 3-7.

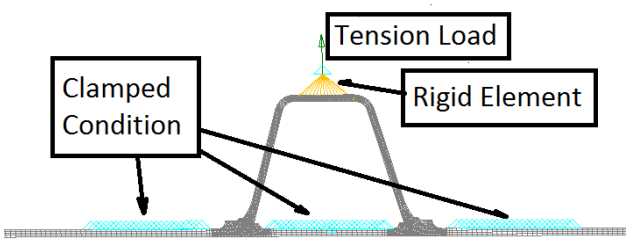

Figure 3-7 Finite Element Mesh for U-Stinger Pull-Off Analysis, full model (left)

The fusion zone for the finite element model was recreated from the micrograph provided by IWS. It was not possible to clearly see the extent of the Heat-Affected Zone (HAZ) in the micrograph, so it was modeled with the same extent used for the L-stringers in WP2

3.2.3. Boundary Conditions

The model was constrained with clamped conditions matching the U-stringer test configuration used by IWS.

3.2.4. Results

Al-Li-as-welded

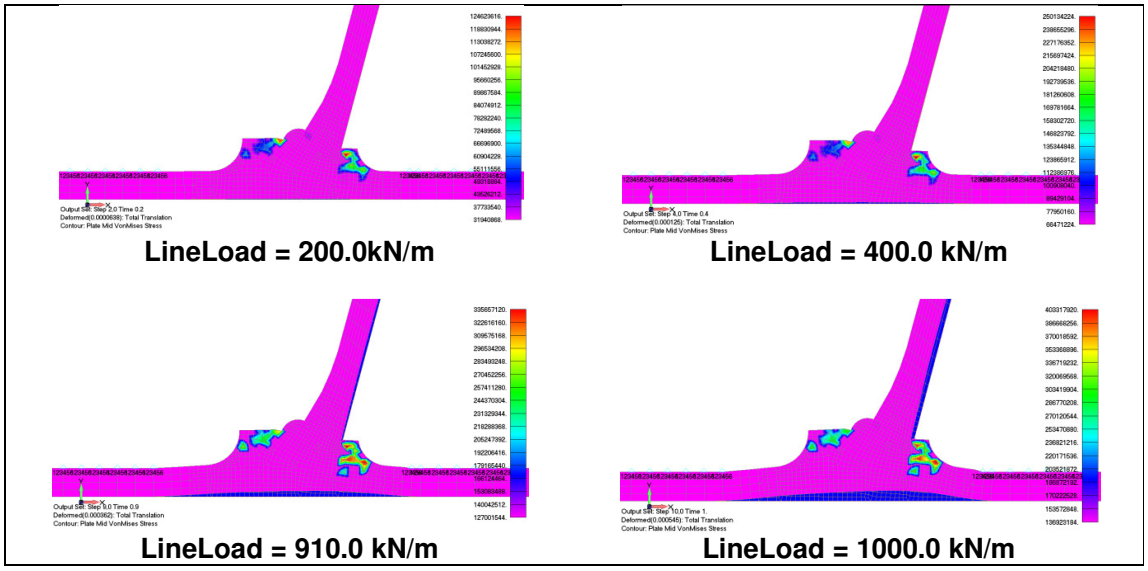

Figure 2-8Von Mises Stress Plots - Al-Li / as welded – U-Stringer

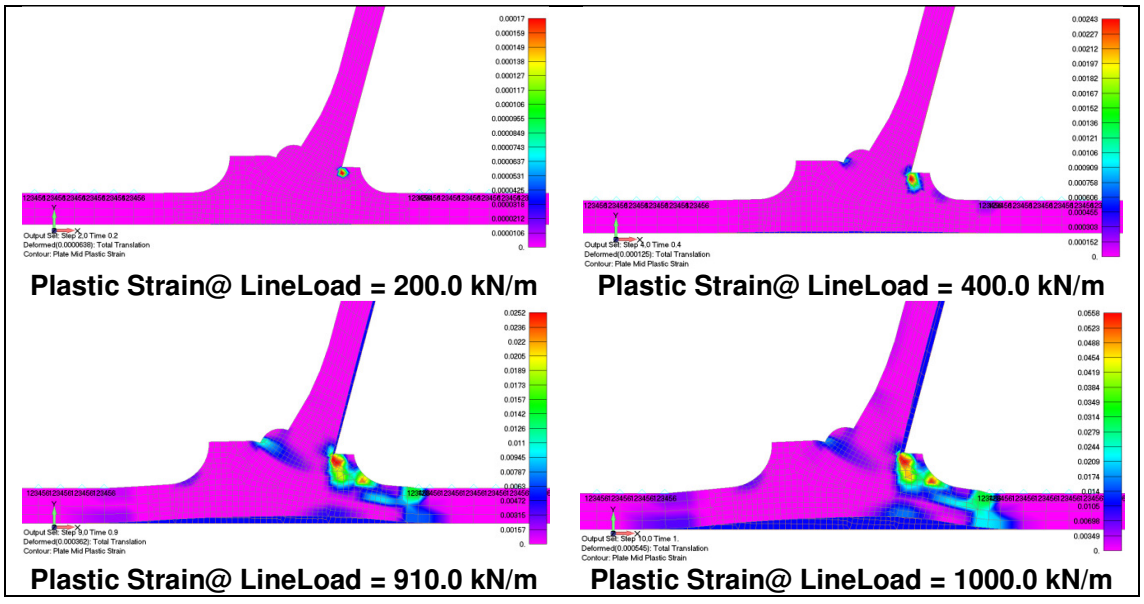

Figure 3-9Plastic Strain Plots - Al-Li / as welded – U-Stringer

Al-Mg-Si-PWHT

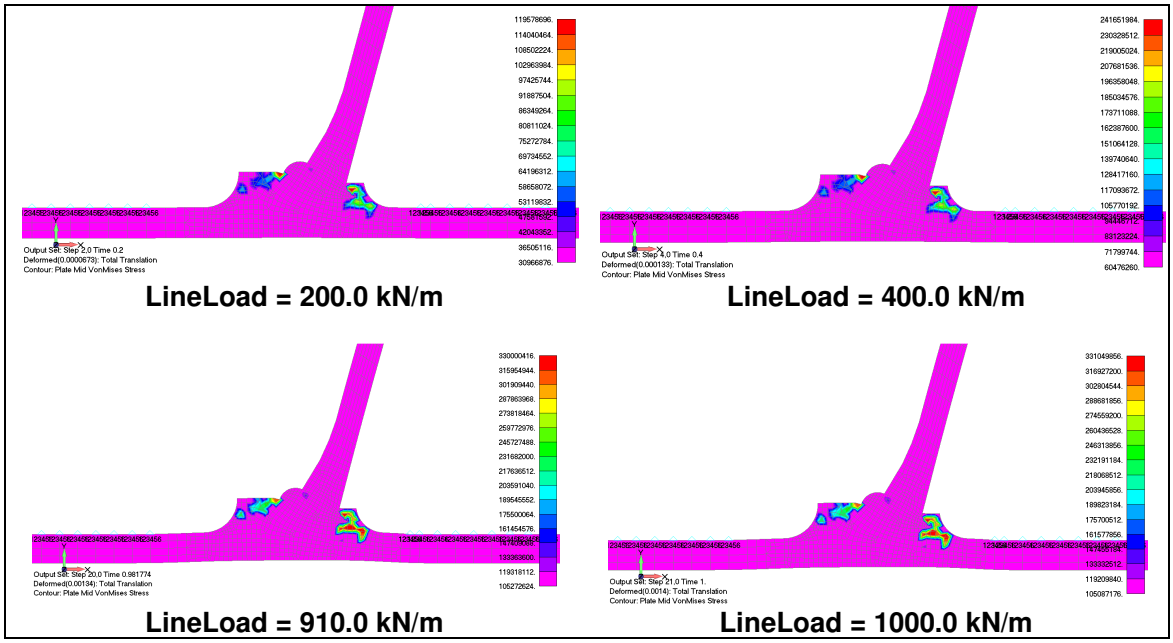

Figure 2-10Von Mises Stress Contour Plots - Al-Mg-Si-PWHT – U-Stringer

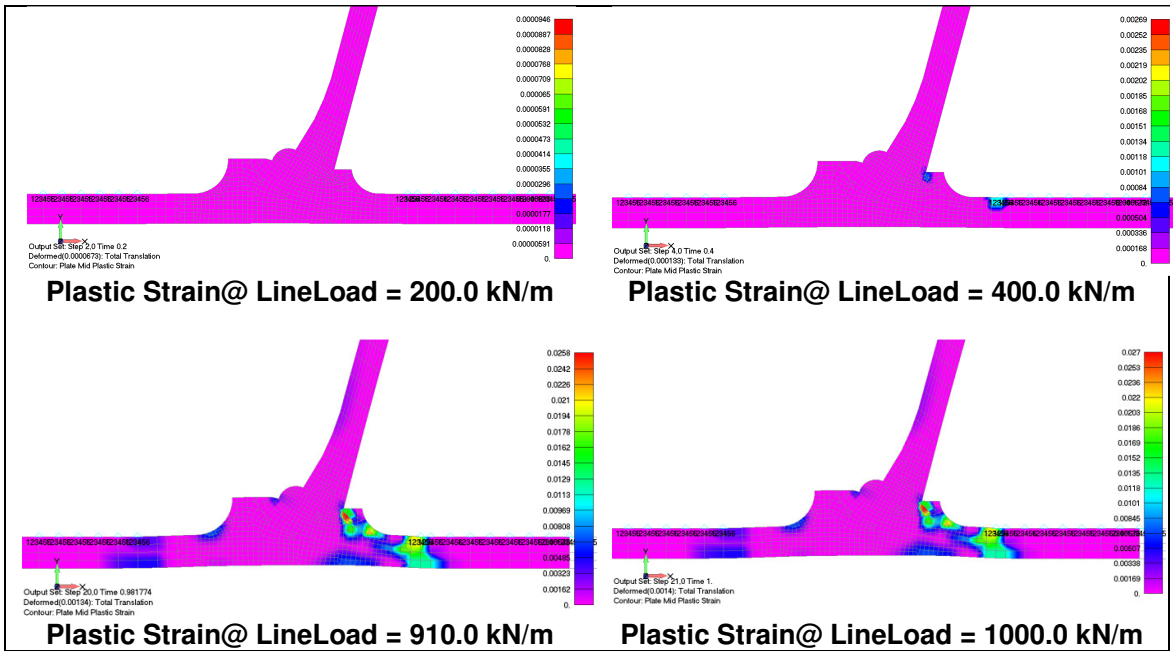

Figure 3-11Plastic Strain Plots - Al-Mg-Si-PWHT – U-Stringer

4. 3D FEM Analysis of Reference Structure

Material data

For the 2D elements case, two models with different material properties were analysed. The materials used for the two FEM models of the reference structure were named R1 and. The R1 was the original baseline design provided by Fraunhofer IWS for the reference structure. After the preliminary results of the LBW analysis Fraunhofer IWS expressed an interest in an alternative reference structure (R2) based on the Al-Mg-Si material.

Model	Material		Heat Treatment
	Stringer	Skin	
R1	Al-Li 2198	Al2024	as welded
R2	Al-Mg-Si 6013 T6		as welded

Table 4-1 Materials used for 3D FEM models of the Reference Structure

For the 3D elements case, only the R1 model was analysed. Therefore only the R1 model is shown here for better comparison.

4.1. 3D FEM Analysis of Reference Structure using 2D elements

4.1.1. General description of FEM Model

The model is composed of CQUAD4 elements, which are commonly referred to as “plates” or “(thin) shells”. This type of element is commonly used for aerospace structures with stiffened monocoque construction.

4.1.2. Initial Imperfections

Initial imperfections were modeled as pre-deformations corresponding in shape to the first eigenmode of a linear buckling analysis using the SOL105 solver in NASTRAN. This modeshape was scaled to give maximum displacements specified as percentage of the skin thickness with the values - 0%, 50%, 100%, 200% and 350%.

4.1.3. Analysis Results

The results are summarized in Table 4-2.

		Pre-deformation (percentage of skin thickness)				
		0%	50%	100%	200%	350%
Failure Load (Collapse) [N]		200222	200437	200250	200096	200075
ε plastic [%]	Skin	0.997	0.783	0.823	0.926	0.968
	Stringer	2.192	1.103	1.059	1.090	1.003
Rivet Max.Axial Load [N]		1422	1248	1297	1283	1193
Rivet Max.Shear Y Load [N]		797	897	922	941	906
Rivet Max.Shear Z Load [N]		1277	932	928	921	899
Inter-rivet Buckling Load [N]		153710	154017	152624	149891	146625

Table 4-2 Summary of 3D FEM Results for Reference Structure

The 3D FEM analysis of the reference structure resulted in a collapse load of between 200.075 KN and 200.437 KN, depending on the assumed magnitude of initial imperfection.

The plastic strain levels in the skin and stringer were well below the respective ultimate values for all load steps, therefore the failure is not due to rupture.

Close-up examination of the deformed shape shows that inter-rivet buckling occurred in regions of the skin subject to high compression.

The collapse involves crippling of the stringers, starting with the stringer on the right of the image.

The plastic strain levels at collapse are shown in Figure 4-1.

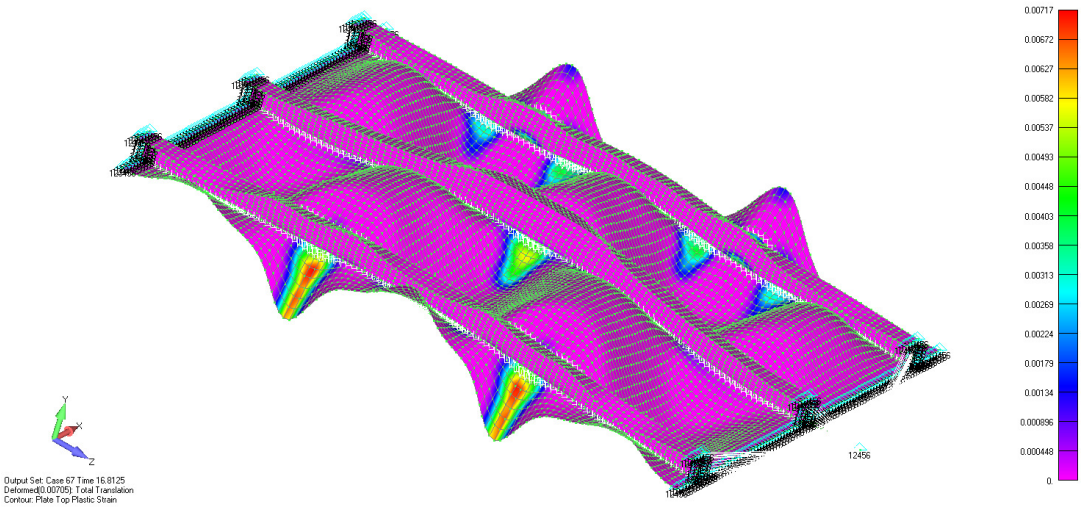

Figure 4-1 Reference Structure Plastic String at Collapse (100% predef. case)

Relatively low levels of plasticity were found and the ultimate strain was not reached, meaning that the structure's collapse load is not determined by rupture of the material.

The highest plastic strains were located at roots of the stringers and in the skin at locations coinciding with the high rotations of the stringer cross-section.

4.2. 3D Analysis of Reference Panel using 3D elements

4.2.1. Results

The deformed shape and von mises stresses at rupture are shown in Figure 4-2.

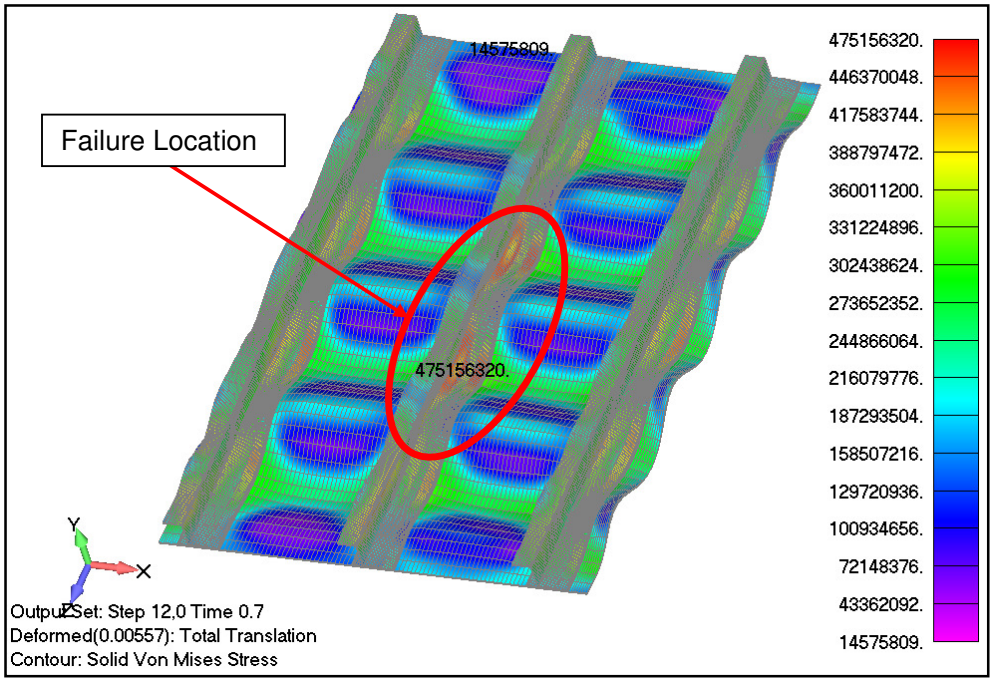

Figure 4-2 Von Mises Stresses and Displacement field at Rutpure of Solid Analysis of the Reference Structure

The failure mode of the model is a global collapse, or more precisely, Euler Johnson buckling with inter-rivet buckling amplified by substantial gapping of the stringer-skin junction.

At the highest load reached in the analysis, no element in the model reached its ultimate plastic strain. Although the material did not rupture, if the analysis was continued, eventually rupture would be reached.

Failure occurs at an applied load of 228.75kN, at which point the panel buckles.

The deformation shape and strain distribution at this load point is shown in Figure 4-3.

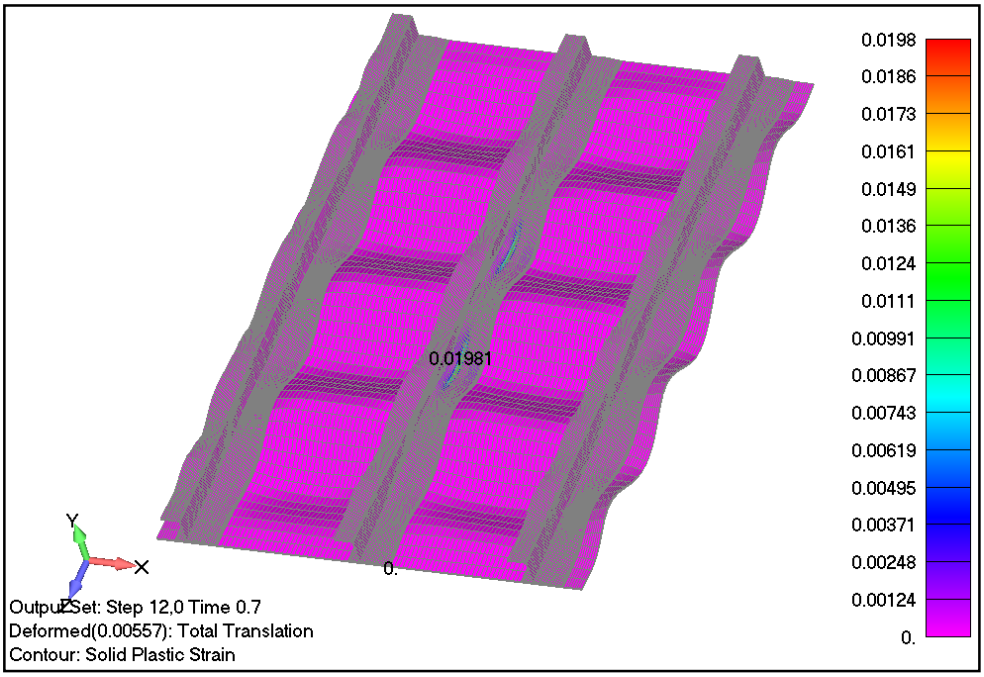

Figure 4-3 Plastic Strain Distribution at Failure – Al-Li Riveted L-Stringer Panel with 3D Solid Elements (Section View)

The buckling mode is symmetric about the central stringer, with 3½ buckling waves along the longitudinal axis of each skin panel. This differs from the buckling modeshape of the shell element model. That model had a buckling mode that was anti-symmetric about the central stringer and less buckling waves in the longitudinal axis.

5. 3D FEM analysis of LBW Structure

Material data

For the 2D elements case, three different materials were considered for the LBW structure. These are shown in Table 5-1.

Material	Heat Treatment	Model
Al-Li 2198	as welded	W1
Al-Mg-Si 6013 T6	as welded	W2
Al-Mg-Si	PWHT	W3

Table 5-1 Summary of Materials used for 3D FEM Models of LBW Sttructure

For the 3D elements case, only the W1 model was analysed. Therefore only the W1 model is shown here for better comparison.

5.1. FEM Elements Analysis of LBW Structure using 2D elements

5.1.1. FEM Model

The approach taken for the 3D FEM of the LBW structure was essentially the same as for the reference structure, except for the modeling of the joints between the stringers and the skin, and the material properties. The weaker weld area was modeled by elements with properties corresponding to the fusion zone. This was applied to the bottom row of elements on each stiffener as shown in Figure 5-1.

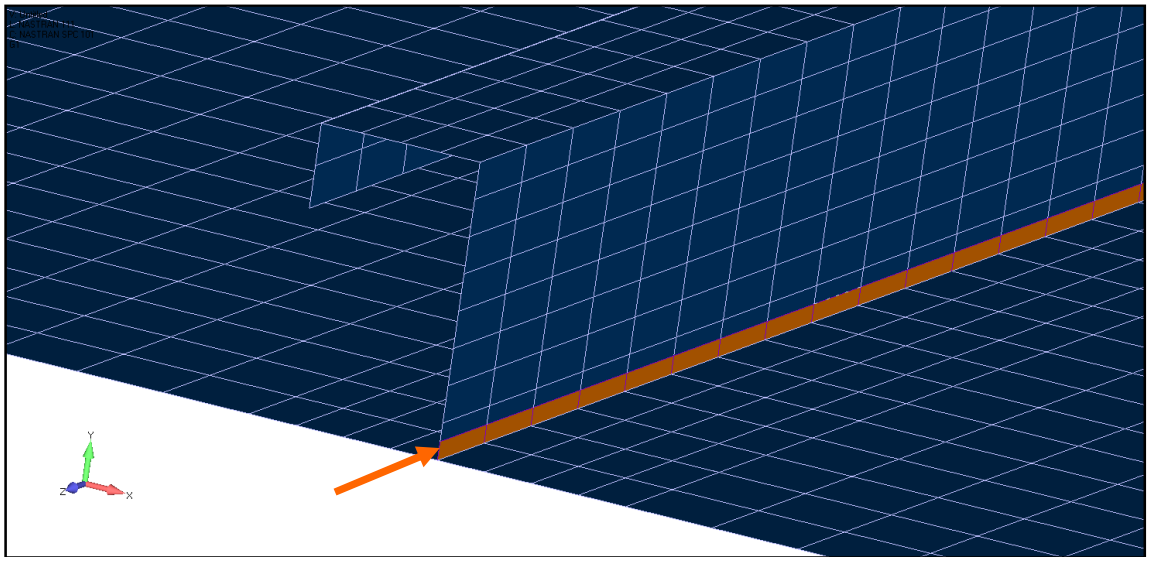

Figure 5-1 Elements Representing the Weld Area for 3D FEM of the LBW Structure

5.1.2. Analysis Results

The results of the 3D FEM analysis of the LBW structure are summarized in Table 5-2.

		Pre-deformation scale				
		0%	50%	100%	200%	350%
Failure Load (Collapse) [N]		226005	225891	225842	225724	225712
ε plastic [%]	Base Material	0	0.00121	0.00264	0.00294	0.00319
	Weld Zone	3.867	3.839	3.761	3.577	3.298

Table 5-2 3D FEM Analysis of LBW Structure Results Summary

The collapse load was in the range 225.712 KN to 226.005 KN depending on the assumed magnitude of the pre-deformation. In each case, the plastic strain level in the fusion zone reached the ultimate plastic strain at the same load step as the collapse.

The failure is initiated by rupture of the weld zone leading to lateral buckling of one of the stringers.

The plastic strain distribution at the collapse load for the 100% pre-deformation case is shown in Figure 5-2. A local zoomed image of the plastic zone at the base of the stringer is shown in Figure 5-3.
Only the elements in the weld zone show any plasticity.

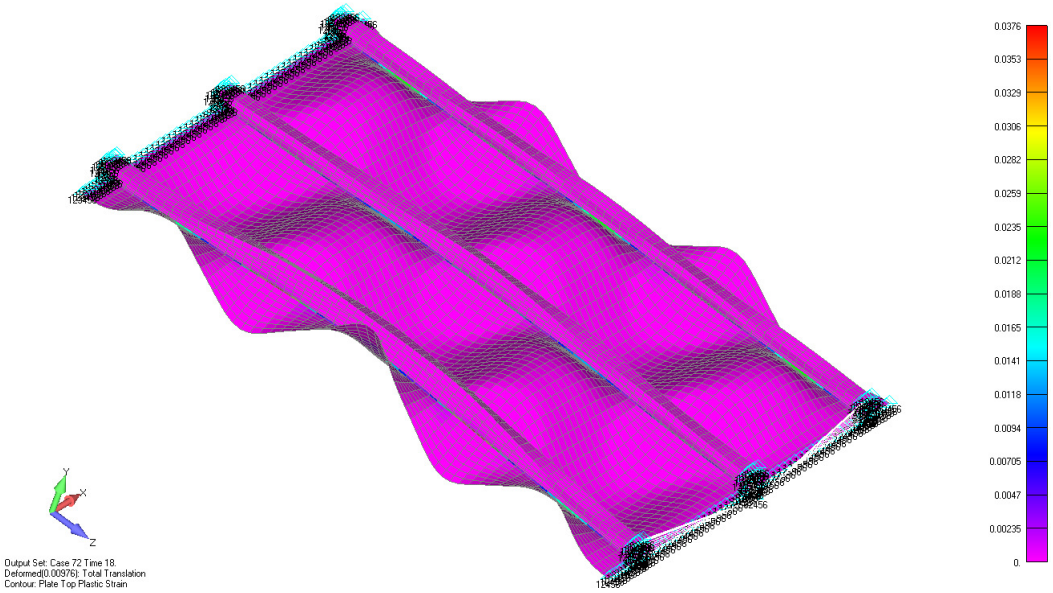

Figure 5-2 Plastic Strain for LBW Structure at Collapse Load

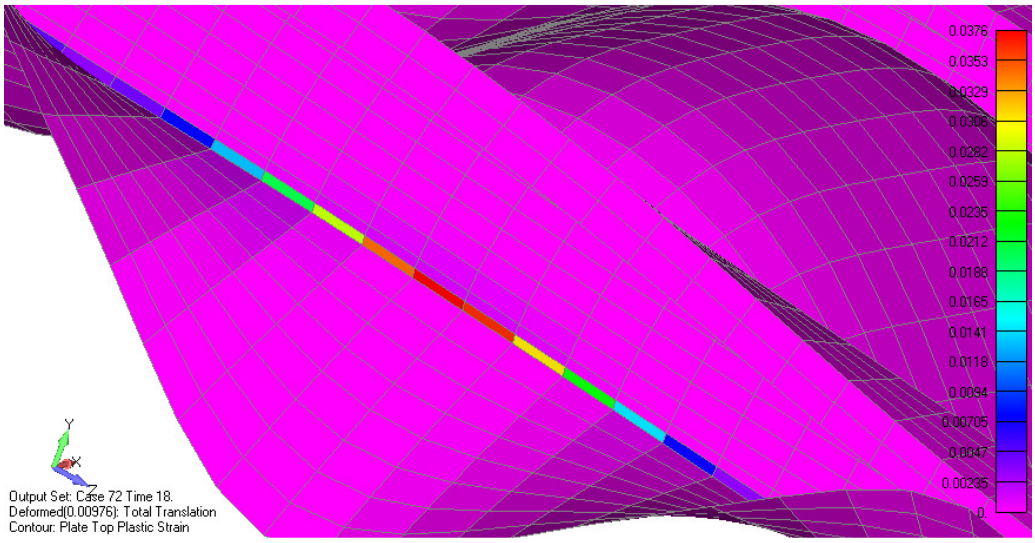

Figure 5-3 Plastic Strain for LBW Structure at Collapse Load – Zoomed In

5.2. FEM Elements Analysis of LBW Structure using 3D elements

5.2.1. Results

The deformation shape and von Mises stresses at rupture are shown in Figure 5-4.

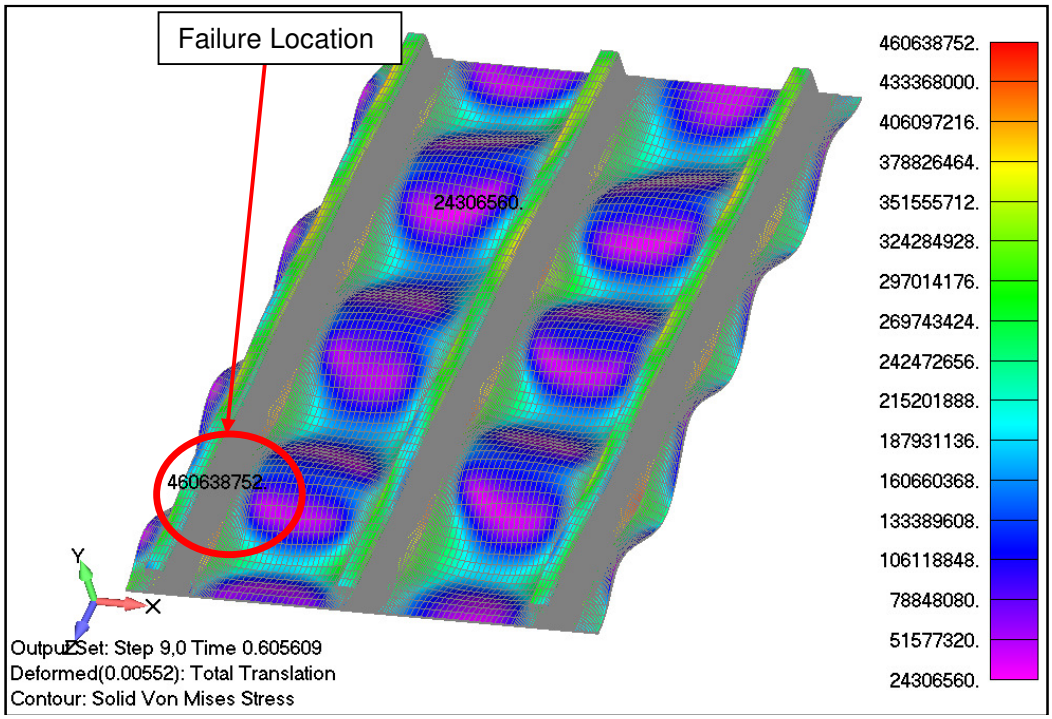

Figure 5-4Von Mises Stresses and Deformation at Rupture of Solid Element Model of LBW Structure

Due to numerical convergence problems, the solution did not reach the failure load. However, the final failure would be expected to occur predicted due to rupture in the fusion zone of the weld seam at the stringer root on the left side of the panel. The final failure load would be expected to occur at a load only slightly higher than the final load step reached by the analysis.

The local detail of the plastic strain and deformation shape is shown in Figure 5-5, which is a transverse cross-section through the model at the location of maximum stress indicated in Figure 5-4.

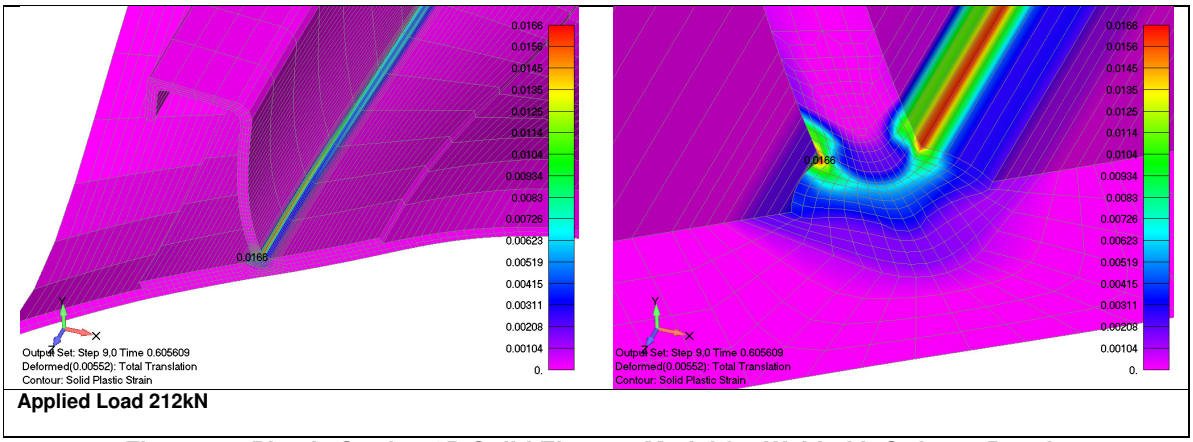

Figure 5-5 Plastic Strain - 3D Solid Element Model for Welded L-Stringer Panel

The right side of Figure 5-5 shows that the stringer root shows high plasticity on both of its sides. This phenomenon is known as a “plastic hinge”, and it indicates that the stringer has relatively low resistance to lateral bending. The left side of Figure 5-5 shows that the stringer is rotating significantly at the weld seam, and this rotation has a destabilizing effect on the structure’s global buckling pattern.

Based upon the plastic strain results and deformation shape in Figure 5-5 it is possible to conclude that the failure load would be in the range 212kN to 250kN.

The problems with numerical convergence are probably due to changes in the global buckling modeshape, whereby the structure wants to ‘snap through’ (jump) to a new modeshape with a lower energy state. Such effects were successfully captured by the SHELL element models in the Intermediate Report, which were obtained with a smaller step size. However, due to the higher computational effort associated with these large SOLID element models, it was not possible to obtain such results within the manpower and time remaining for this project.

6. Conclusion

6.1. Mass Comparison

Mass budgets were produced for both structures studied in this report and the results are summarized in Table 6-1.

		Total Volume (m^3)	mass density (Kg/m^3)	Weight (Kg)
Reference Structure	stringer	2.05E-04	2629.6	1.993
	skin	5.25E-04	2768.0	
LBW Structure	total	6.78E-04	2629.6	1.783

Table 6-1 Mass Comparisons

The reference structure is slightly heavier than the LBW structure.

6.2. General Remarks on Accuracy of Results

The FEM models developed for this project, like for all numerical analysis, feature certain assumptions.

In general, the error margin expected for such FEM models should be no greater than about 5% for tension-type failure modes with well-defined material and geometric properties. Due to the uncertainties in material properties of the weld seam, this error margin would be expected to be somewhat higher, probably around 10%.

In the case of 3D FEM analysis of compression buckling type failure modes there is more uncertainty. This arises from imperfect knowledge of the initial imperfections and internal pre-loads in the structure induced during its manufacturing. Although detailed studies of such effects are possible, it was beyond the scope of this project. Considering this, the error margin for the 3D FEM compression models is considered to be about 10%.

The classical method applied for strength predictions of the compression panels is intended to be conservative, taking into account all manufacturing imperfections, andtherefore the classical results should represent the lower bound of the error margin. However, since it is based on proprietary knowledge determined empirically by tests, no information is available on the margin that is present in the classical method. Thus, it is difficult to directly compare the classical and FEM results.

6.3. 2D Pull-Test Analysis Results

Results of the 2D pull-test FEM analyses are shown in Table 6-2.

Stringer/Weld Type	Material	Heat Treatment	Rupture Effective Stress [MPa] / Failure Location				Rupture Line Load [kN/m]
			SOL106		SOL600		SOL600
L-Stringer / 1	Al-Li	as welded	531	Fusion Zone	479	Fusion Zone	766.4
L-Stringer / 2	Al-Li	as welded	475	Fusion Zone	450	Fusion Zone	720.0
L-Stringer / 1	Al-Li	PWHT	609	Base	575	HAZ	920.0

				Material			
L-Stringer / 1	Al-Mg-Si	as welded	418	Base Material	433	HAZ	692.8
L-Stringer / 1	Al-Mg-Si	PWHT	410	Base Material	423	Base Material	676.8
U-Stringer	Al-Li	as welded	-		-	Base Material	950.0
U-Stringer	Al-Mg-Si	PWHT	-		-	Top of Stringer	541.3 [1]

Note: 1. This configuration first failed at the top of the stringer. The weld seam remained intact until at least 1000.0kN/m

Table 6-2 2D Pull-Test Results

6.4. Panel Compression Analysis Results

Three distinct analysis methods were used for the 3D Panel Compression Analysis;
- Classical,
- FEM with SHELL elements, and
- FEM with SOLID elements.

Since the three methods involved quite different analytical approaches, the results are first discussed individually in the following sub-sections, and then finally, sub-section 6.4.4 discusses the comparisons between the methods.

6.4.1. Classical Method

Results of the panel compression analyses by classical methods are shown inTable 6-3. Full details of these were presented in Sections 2.2 and 3.2 of the Intermediate Report.

Structure	Model	Materials (Stringer/Skin)	LOAD (kN)			Failure Mode
			Skin Buckling	Plasticity Onset	Collapse	
Reference	R0	Al-Li 2198 / Al2024	48.008	-	140.308	Global Panel Buckling at load reduced by inter-rivet buckling
LBW	W0	Al-Li 2198 as welded	66.686	-	178.892[1]	Global Panel Buckling

Note: 1. The classical method does not consider the weaker material properties at the weld seam, and might be unconvervative

Table 6-3 Panel Compression Results by Classical Method

The classical method that was employed in this project is intended for design purposes, and thus includes a number of empirical relations based on test results. Since the methodology was developed for design purposes, it is possible that its results are conservative for certain panel design configurations.

One important limitation of the classical method is that it does not include the possibility of failure by rupture at the weld seam. This means that the calculated failure load for the welded structure W0, might be unrealistically high (i.e. unconservative).

Ignoring any possible weld seam rupture, the classical results show that the specified LBW panel, W0, was substantially (28%) stronger than the Reference panel, R0.

6.4.2. SHELL Elements

Results of the panel compression FEM analyses with SHELL elements are shown inTable 6-4. Full details of these calculations were presented in Sections 2.3 and 3.3 of the Intermediate Report.

Structure	Model	Materials (Stringer/Skin)	LOAD (kN)			Failure Mode
			Skin Buckling	Plasticity Onset	Collapse	
Reference	R1	Al-Li 2198 / Al2024	45.434	143.75	200.222	Global panel buckling at load reduced by inter-rivet buckling and gapping at stringer-skin junction
	R2	Al-Mg-Si 6013 T6	42.940	131.250	187.523	Global panel buckling at load reduced by inter-rivet buckling
LBW	W1	Al-Li 2198 as welded	41.714	62.500[2]	226.005[2]	Weld zone rupture leading to separation of left stringer[2]
	W2	Al-Mg-Si 6013 T6 as welded	39.257	56.25[2]	188.086[2]	Global panel buckling at load reduced by plasticity in weld seam[2]
	W3	Al-Mg-Si PWHT	39.282	81.25[2]	180.457[2]	Global panel buckling at load reduced by plasticity in weld seam[2]

Note: 2. The SHELL element models do not accurately represent the behaviour and strength of the weld seam

Table 6-4 Panel Compression Results by 3D FEM with SHELL Elements

The SHELL element models of the reference panels, R1 and R2, predicted failure by global panel buckling. The effects of the inter-rivet buckling and gapping between skin and stringer were accurately represented by these models.

The SHELL element models of the two welded Al-Mg-Si panels W2 and W2 predicted failure by global panel buckling, although plasticity was present in the weld seam.

The SHELL element model W1 predicted failure by rupture of the weld seam, which would lead to separation of the stringer. The different failure mode of W1 can be attributed to the relatively low strength of the Al-Li 2198 material in the ‘as welded’ state.

It should be noted that the SHELL element modes included only a crude representation of the weld seam (see Figure 3-50 of the Intermediate Report), and as such only give an approximate prediction of weld seam rupture or the initiation of plasticity in the weld seam. The error margin on such results could be as high as 20%.

All SHELL element results were calculated with assumed initial imperfections in the shape of the first linear buckling mode. A more comprehensive investigation of all possible initial imperfections is recommended for actual design projects. However, the results clearly showed an early onset of skin buckling followed by eventual buckling of the stringers. This indicates that the selected panel geometries are rather insensitive to initial imperfections.

6.4.3. SOLID Elements

Results of the panel compression FEM analyses with SOLID elements are shown in Table 6-5. Full details of these were presented in Sections 4.2.1 and 5.2.1of this report.

Structure	Model	Materials (Stringer/Skin)	LOAD (kN)			Failure Mode
			Skin Buckling	Plasticity Onset	Collapse	
Reference	R1'	Al-Li 2198 as welded	60.000	150.000	210.000 [3]	Global panel buckling at load reduced by inter-rivet buckling and gapping at stringer-skin junction
LBW	W1'	Al-Li 2198 as welded	97.982	97.982	211.963 [3][4]	Weld zone rupture leading to separation of stringer

Notes: 3.No sensitivity study conducted for initial imperfections
4. Actual failure load was not reached due to numerical convergence problems. Failure load could be as high at 250kN

Table 6-5 Panel Compression Results by 3D FEM with SOLID Elements

The failure modes was predicted by global panel buckling,

6.4.4. Comparison of Panel Compression FEM Methods

The SHELL element and SOLID element models both have their respective strengths and weaknesses, however further work is required before either method can be used for accurate analysis results, suitable for airframe structure certification purposes.

The SHELL element models have relatively few elements and thus provide a solution time of only a few hours on the typical modern computers used for this project. The SHELL elements are suitable for modeling global effects in the large regions of the panels, but the representation of the weld seam does not give sufficient accuracy for local failures.

The SOLID element models can provide sufficient accuracy for local failures, but this comes at a high computational cost, since it is impossible to predict in advance where the failure will occur. The high computational costs also make a thorough investigation of the effects of initial imperfectionsvery time consuming.

6.4.5. Relevance of 2D Pull-Test Specimens for 3D Panel Compression

The 2D pull-test specimens showed failure modes with almost pure tension in the weld seam. This differs from the 3D panel compression specimens which showed failure by lateral bending of the stringer root at a load weakened by plasticity in the weld seam (see Figure 5-5 of this report). The difference between these local failure modes means that the results of the 2D pull-test specimens cannot be directly used to predict the strength of the 3D compression panels.

The 2D results do however permit an assessment of the relative strength of the different materials and heat treating options of the welded joint, and it is likely that a design that performs well in the pull-test loading will also show good resistance to stringer rotation in 3D panel compression loading.

The failure of 3D compression panels with "U" shaped stringers was not considered in this project but it is possible that such panels have higher resistance to stringer rotation, and hence higher panel compression strength relative to "L" stringers.

7. References

[1] AOES-RP-21062010, FusDesOpt Intermediate Report – Analysis of Reference Structure and Impact of Laser Beam Welding, Rev 1, 21/6/2010.

[2] Email from Dirk Dittrich, Subject: “AW: Materials for U-stringer “,17/09/2010 3:39 PM